

Damien Servant  
Image Processing & Project Engineer

# DT26X - LiDAR performances



# Content



<b>INTRODUCTION</b>	<b>p.3</b>
<b>VECTOR AND PAYLOAD</b>	<b>p.4</b>
2.1 Vector	p.4
2.2 Payload	p.4
2.2.1 LiDAR	p.4
2.2.2 GNSS/IMU	p.5
<b>TEST FIELD</b>	<b>p.6</b>
<b>FLIGHTS</b>	<b>p.7</b>
<b>PROCESSING</b>	<b>p.8</b>
<b>RESULTS</b>	<b>p.10</b>
6.1 Point density	p.10
6.2 Measurement accuracy with APX15	p.11
6.3 Measurement accuracy in comparison with high end IMU	p.12
<b>CONCLUSION</b>	<b>p.14</b>



# 2. Vector and payload

## 2.1 Vector

For this study, the DT26X-LiDAR UAV was used. Its main specifications are as follows:

	DT26X LiDAR
Endurance	Up to 2.5 h
Wingspan	3.3 m
Length	1.6 m
Cruising speed	65 km/h
Payload capacity	Up to 4 kg



Figure 1 - DT26X LiDAR

## 2.2 Payloads

### 2.2.1 LiDAR

Delair-Tech chose the VUX-1 UAV LiDAR from RIEGL for its performances:

	VUX-1 UAV
Accuracy	10 mm
Precision	5 mm
Laser Measurement Rate	Up to 500,000 meas./s
Laser Wheel Speed	Up to 200 rotations/s
Max Measuring Range	170m (for 500,000 meas./s and a reflexivity of 20%)

The Riegl LiDAR is used in combination with the RiProcess software package.

## 2.2.2 GNSS/IMU

Applanix has been recognized in the aerial mapping field for many years, and their "APX-15 UAV" GNSS/inertial system was chosen for the DT26X-LiDAR UAV.

For a specific client, a custom UAV was developed based on an AP20 GNSS/inertial system with higher performance at the cost of a heavier payload.

The position and attitude characteristics, once the data have been post-processed with Applanix POSPac software, are specified as:

	APX-15 UAV	AP20
Position	2 to 5 cm	2 to 5 cm
Velocity	15 cm/s	5 cm/s
Roll & Pitch	0.025°	0.015°
True heading	0.08°	0.05°
Inertial Navigation System (INS)	Integrated Solid-state MEMS inertial sensor	External Inertial Measurement Unit
Weight (with antenna)	225 grams	1215 grams

This system is autonomous, i.e. its results can be obtained without establishing any base on the ground, thanks to the permanent network used by Applanix for post-processing and calculating the trajectory. It uses carrier-phase tracking, in addition to differential and bi-frequency technology. Furthermore, the GPS data is fused with the IMU data.

# 3. Test field

A test zone was defined as a use case for an electric power distributor who wanted to evaluate the effectiveness of a LiDAR flown on a DLT26X UAV for infrastructure monitoring during the installation of new conductors on electric pylons.

The area consisted of a rectangular power-line corridor, approximately 3600 x 120 meters in size, containing 8 electric pylons.

Six control points were measured on the ground thus guaranteeing the absolute accuracy of the measurements.

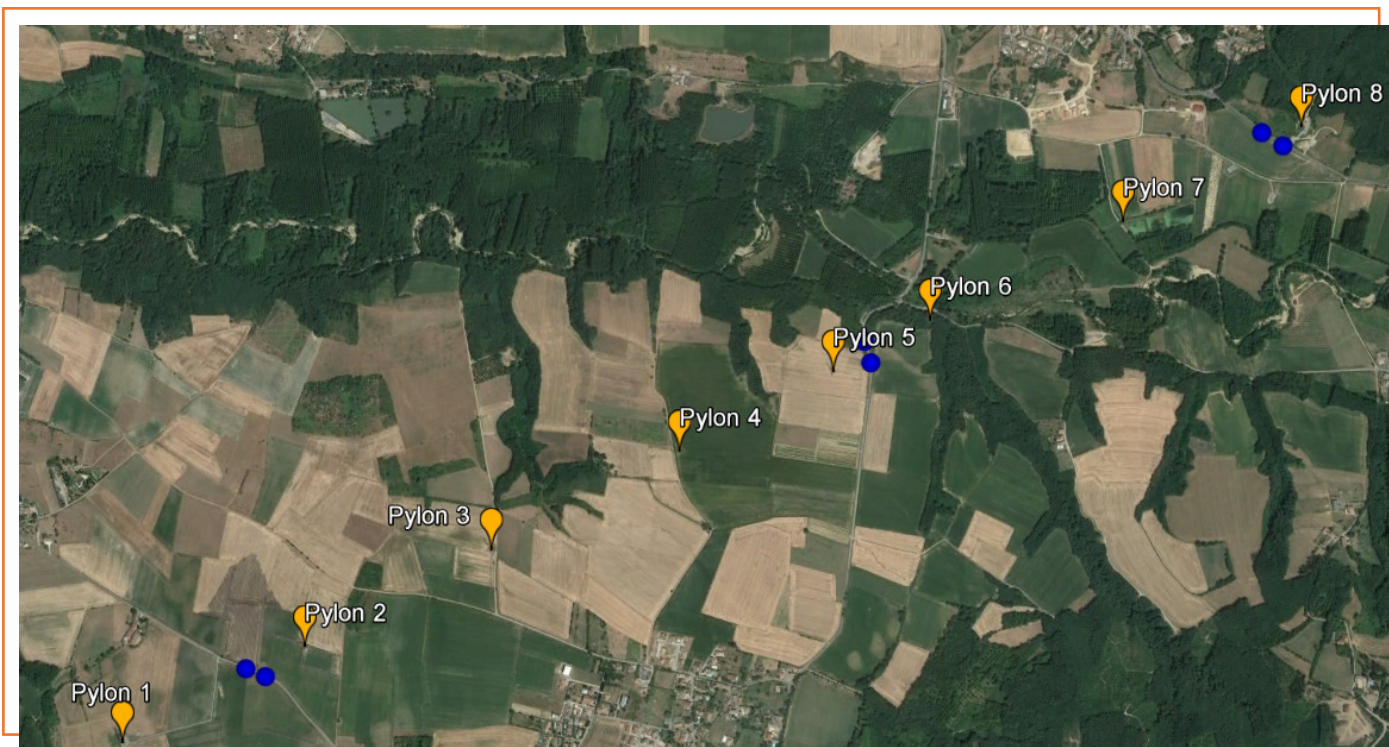


Figure 2 - Test field with electric pylons (orange) and GCPs (blue) - ©Google Earth

# 4. Flights

Delair-Tech conducted a series of 4 tests over a period of 3 days:

N	Date	UAV & Payload
1	2016 August 18th	DT26X-LIDAR with APX15
2	2016 August 24th	DT26X-LIDAR with APX15
3	2016 September 12th	DT26X-LIDAR with APX15
4	2016 September 12th	DT26X-LIDAR with AP20

Two different payloads were tested on the last day under the same conditions: first with the APX15 and then with the AP20.

For all flights, the DT26X was operated with the same parameters:

Parameter	Characteristics
Speed	18 m/s
Altitude	120 m
Recording trajectory	Two-way in a security corridor around the electric pylons
LIDAR pulse repetition rate	550 kHz
LIDAR Scan speed	110 rotations/s

The flight trajectory of the DT26X-LiDAR for the last day was as follows:



Figure 3 - Flight Trajectory for day 3 (in red the useful part for the LiDAR) - ©Google Earth

# 5. Processing

After the flight, the Applanix navigation data were post-processed using POSPac software in order to integrate the lever arms and calculate the precise trajectory (X,Y,Z,O,P,K). The “smart base” method from Applanix was used to improve the localization accuracy using 6 GNSS reference stations.

After the navigation data processing, the LiDAR raw scan data were processed and merged with the trajectory data from the GNSS/INS system using the Riegl RiProcess software. This step generates the georeferenced 3D point cloud of the field. These data were then classified into categories: fields, pylons, power lines...

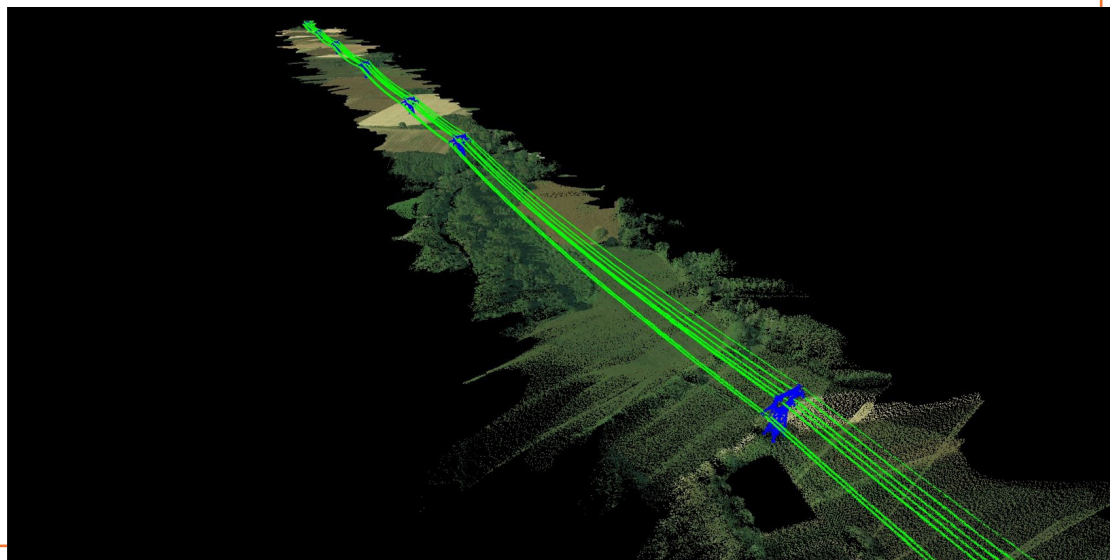


Figure 4 - Georeferenced 3D point cloud with the 3 categories

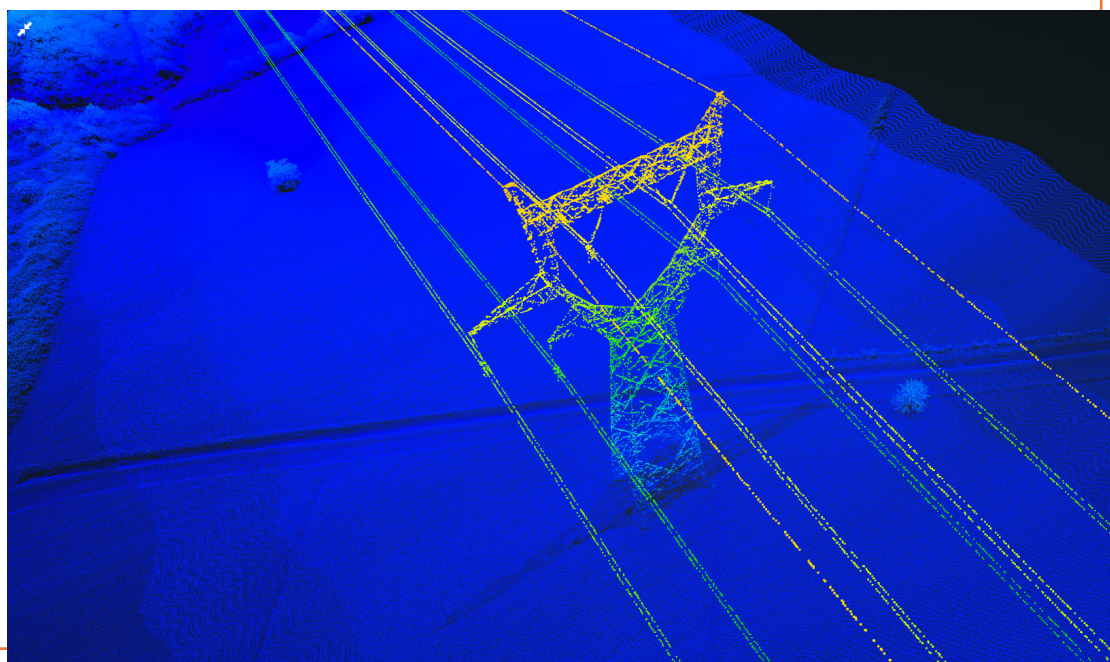


Figure 5 - Extract of the 3D point cloud with a height colormap

To compute the accuracy of the LiDAR measurements, the points of the power line between the 6th and 7th electric pylons were extracted. The points were converted from the Lambert-93 coordinate system to the following electric pylon reference frame:

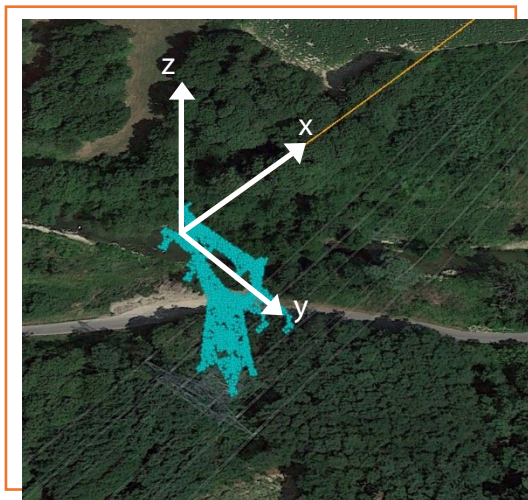


Figure 6 - Electric pylon reference frame for the processing

The power line was then modeled using 2nd order polynomials along the Y and Z axes which fit the selected point cloud in a mean squared sense:

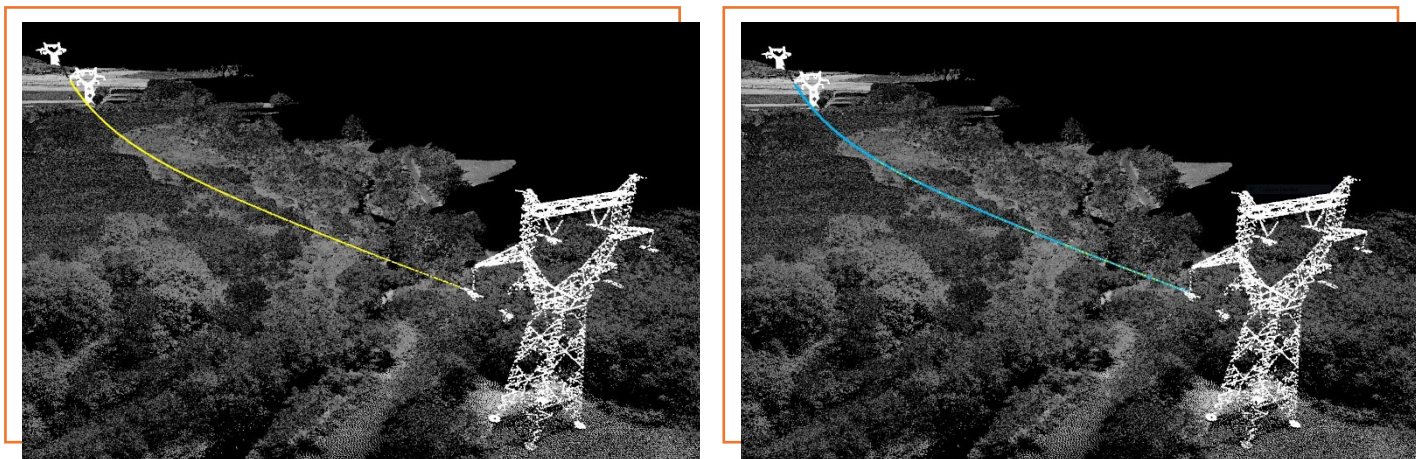


Figure 7 - Power line modeling in yellow and the related LiDAR points in blue

This dataset will be used to compute the measurement dispersion around the modeled power line.

# 6. Results

The test flights were conducted over three days. Every day the wind conditions changed a lot, as measured by the DT26X:

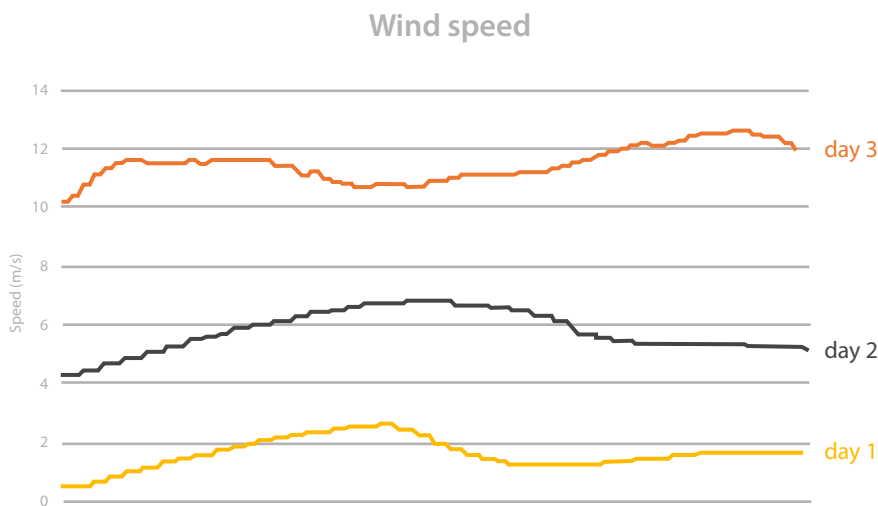


Figure 8 - Wind conditions during tests

While the flights during the first two days took place under good wind conditions, the one during the last day was performed with stronger and more turbulent wind. The flight went ahead without any problem, but the wind condition did affect the measurements presented in the following paragraphs.

## 6.1 Point density

According to the configuration parameters applied to the LiDAR and the DT26X for these flights, the theoretical ground points density was 75 pts/m<sup>2</sup> for a two-way trajectory above the test field.

The following plot shows that the LiDAR coverage density during a flight is globally consistent with this value of 75 pts/m<sup>2</sup>:

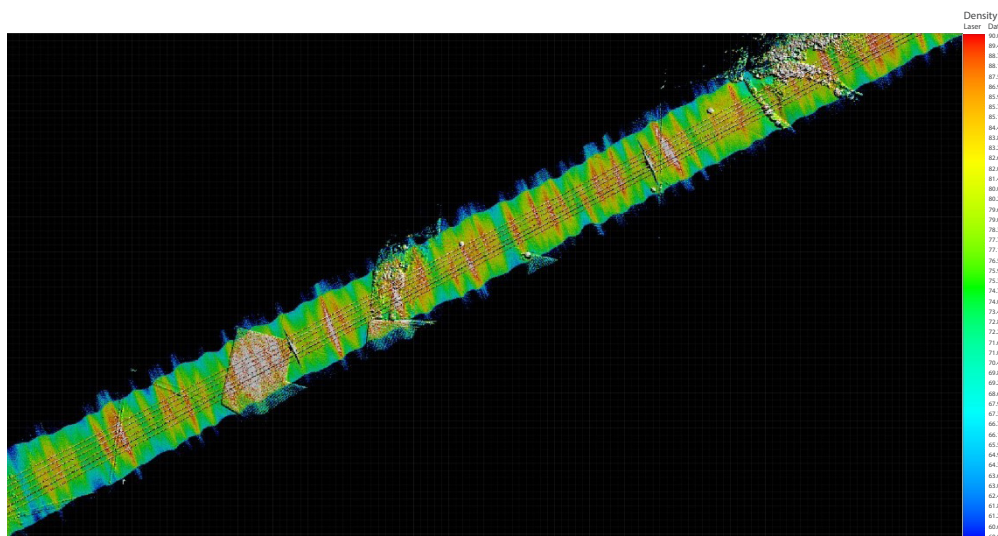


Figure 9 - Point cloud density (day 1)

## 6.2 Measurement accuracy with APX15

The delta between the measured LiDAR point cloud and the numerical modeling of the power line is computed along the Y and Z axes. The error distribution is shown in the following histograms:

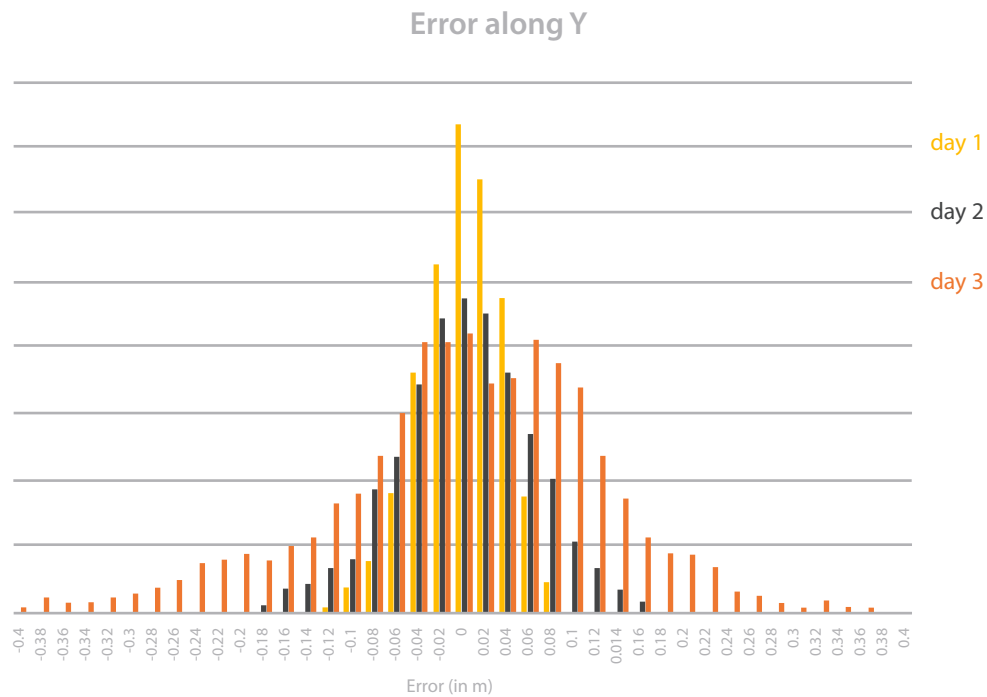


Figure 10 - Measurement error along Y axis

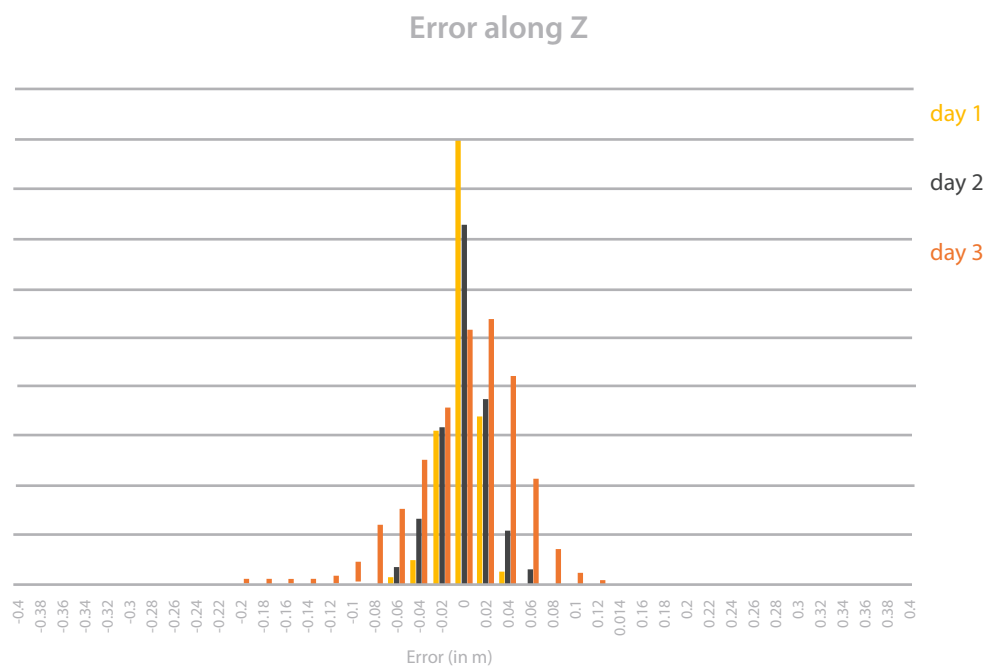


Figure 11 - Measurement error along Z axis

The computed accuracy values with APX15 are summarized in the table below:

Standard deviation (in m)	Day 1	Day 2	Day 3
Sigma along Y	0.036	0.062	0.132
Sigma along Z	0.015	0.022	0.05

They show a direct correlation between the wind turbulence and the LiDAR measurement accuracy as shown on Figure 12:

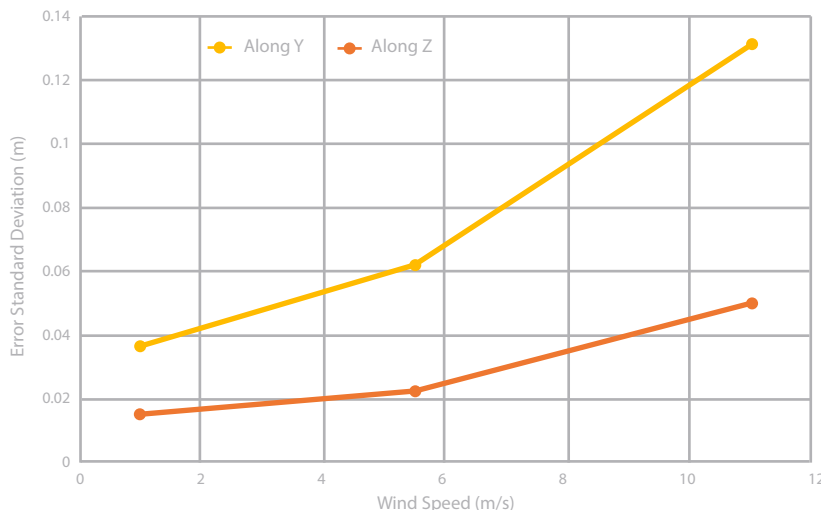


Figure 12 - Impact of wind on LIDAR measurements

### 6.3 Measurement accuracy in comparison with a high end IMU

During the last day, a DT26X-LiDAR custom configuration with a high end AP20 GNSS/IMU flew over the same test field under the same weather conditions with strong and turbulent wind. The delta between the measured LiDAR point cloud and the numerical modeling of the power line was computed along the Y and Z axes. The error distribution is shown in the following histograms:

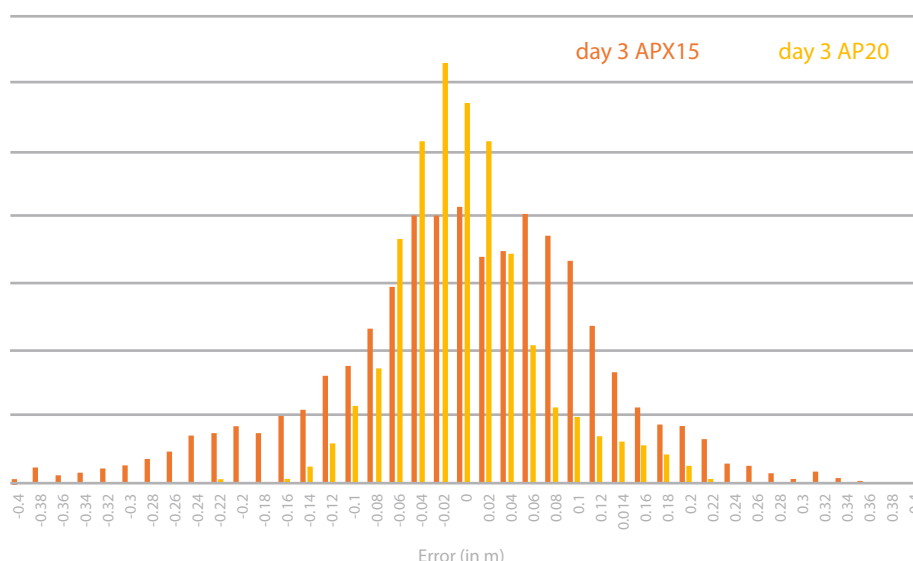


Figure 13 - Measurement error along Y axis

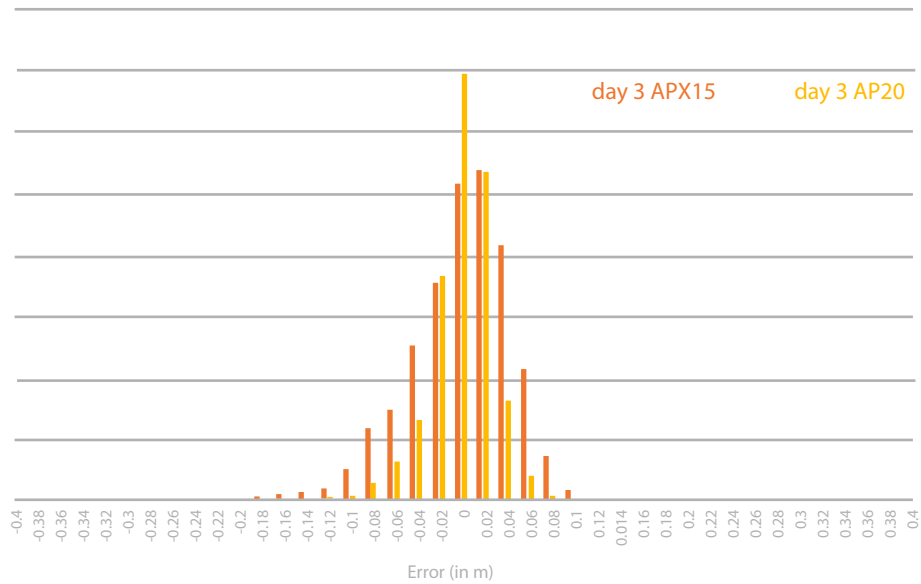


Figure 14 - Measurement error along Z axis

The computed accuracy values are summarized in the table below:

Standard deviation (in m)	Day 3 APX15	Day 3 AP20
Sigma along Y	0.132	0.065
Sigma along Z	0.05	0.028

While the APX15 standard deviation is quite satisfactory for power-line monitoring, note that the AP20 GNSS/IMU error along the Y and Z axes is approximately half that of the APX15.

